Hydration of Sr^{2+} in Hydrothermal Solutions from ab Initio Molecular Dynamics

D. J. Harris* and J. P. Brodholt

Department of Earth Sciences, University College London, Gower Street, London WC1E 6BT, U.K.

D. M. Sherman

Department of Earth Sciences, University of Bristol, Wills Memorial Building, Queen's Road, Bristol BS8 1RJ, U.K.

Received: December 19, 2002; In Final Form: March 17, 2003

Ab initio molecular dynamics calculations have been used to study the dynamical properties of the strontium hydration shell as a function of temperature. At 25 °C, we obtained Sr−O bond lengths of 2.6 Å and a coordination number of 7.5. These are in good agreement with available experimental data. Increasing the temperature to 350 °C led to a decrease in the coordination number to 6.7 and a contraction of the first shell by about 0.1 Å. This is in agreement with the data which predict octahedral coordination of Sr in water at high temperatures. Our calculated Debye−Waller factors also agree well with the experimental values. At higher temperatures (600 °C), we predict that the Sr ion remains in 6-fold coordination.

1. Introduction

The aqueous concentration of Sr in groundwater, hydrothermal solutions, and the oceans is controlled by the precipitation of $SrCO_3$ and $SrSO_4$. The uptake of Sr^{2+} into smectite clay minerals (e.g., montmorillonite), by ion exchange with interlayer Ca^{2+} and Na^{+} ions, will also limit the aqueous concentration of Sr^{2+}. Insofar as these processes retard the mobility of ^{90}Sr, they are of practical significance for the control of nuclear waste and fallout.

The formation of an ordered hydration shell surrounding alkali metal and alkali earth cations is a major contribution to the free energy of ion exchange and mineral dissolution reactions in aqueous solutions. In hydrothermal solutions, changes in the hydration shell with temperature will affect the solubility of minerals and the uptake of cations by ion exchange.

At present, our molecular picture of Sr^{2+} chemistry in hydrothermal aqueous solutions is incomplete. There is, however, considerable data on the hydration of Sr under ambient conditions. Neilson and Broadbent performed neutron diffraction studies on 3m $Sr(ClO_4)_2$ in heavy water.[1] Persson et al. performed large-angle X-ray scattering and EXAFS spectroscopy measurements on 0.82 M $Sr(ClO_4)_2$,[2] while Caminiti et al. performed X-ray diffraction on 2 M $SrCl_2$.[3] Marques et al. performed a combination of X-ray diffraction, Raman, and molecular modeling on concentrated $SrCl_2$ solutions.[4] There is also some work detailing the hydration shell of this ion at higher temperatures including EXAFS work for 0.2 M $Sr(NO_3)_2$ at 385 °C[5] and for 0.1m $SrCl_2$ solutions at 308 °C.[6] The earlier work showed that the number of waters in the first hydration shell of the Sr cation decreases from about eight at ambient conditions to four at supercritical conditions and that the hydration shell contracted very slightly with temperature. The later work[6] also showed a contraction of the hydration shell of about 0.05 Å between 25 and 300 °C; however, at their experimental conditions of 308 °C, the number of waters in the Sr hydration shell dropped from about 7.8 to only 6.2. Classical molecular dynamics simulations were also used to model the effect of temperature and pressure on hydrothermal strontium solutions.[6,7] The simulations of Palmer et al.[7] failed to show any contraction of the first hydration shell, as did the simulations of Seward et al.[6] when using the SPC[8] empirical potential for water. They were, however, able to detect a slight contraction of the hydration shell when using a flexible water potential. They also found, in agreement with their experiments, that the Sr ion remained octahedrally coordinated by water.

To understand the solvation of Sr^{2+} ion in aqueous solutions at high temperature and pressure, we used ab initio molecular dynamics simulations based on density functional theory. The advantage of this approach over classical atomistic simulations is that we do not need to use a potential model that is restricted to pairwise interactions. The disadvantage of using ab initio molecular dynamic simulations is that we cannot sample phase-space well enough to predict an equilibrium speciation. However, we believe that we can understand the local equilibrium of the small system that we are investigating and, in particular, we should be able to understand the local solvation environment of Sr^{2+} and its temperature dependence.[9,10]

2. Modeling

Ab initio molecular dynamics (MD) simulations were performed using the program CASTEP[11] on cells with periodic boundary conditions containing a single cation and 30 water molecules. The cubic cell parameters were set to the ambient temperature values of $a = b = c = 10.628$ Å. Charge neutrality is achieved through the use of a uniform neutralizing background.

The starting configurations for the ab initio MD simulations were taken from a classical MD simulation using the atomistic MD code, Moldy,[12] using pair potentials.[7] The classical simulations were run for 25 ps in order that the starting configuration and velocities for the ab initio calculation were as near as possible to the equilibrium conditions. The starting configura-

* To whom correspondence should be addressed. Phone: +44 (0) 20 76793424. Fax: +44 (0) 20 73887614.

10.1021/jp027772x CCC: $25.00
Published on Web 07/16/2003

TABLE 1: Calculated Internal Water Structure at 25 °C in the Bulk Solution and in the First Hydration Shell[a]

	calcd	exp[16]
O-H (Å) bulk waters	0.991	0.970(2)
HÔH (°) bulk waters	107.6	106.6
O-H (Å) hydrating water	0.991	*a*
HÔH (°) hydrating waters	108.0	*a*

[a] There is no real difference between the two. At 350 °C the average OH bond length is 0.95 Å and HÔH is 107.9°, again with no difference between bulk and hydration shell waters.

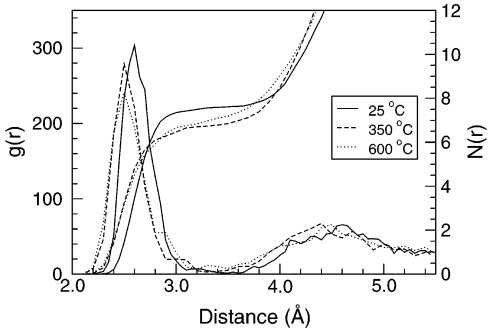

Figure 1. Calculated g(r) and n(r) for Sr−O at 25, 350, and 600 °C.

tions were further relaxed with a short (0.1 ps) ab initio simulation before collecting results.

The ab initio calculations employ the density functional formalism (DFT) using a plane wave basis set with Vanderbilt ultrasoft pseudopotentials to approximate the interactions between core and valence electrons. A plane wave cutoff of 380 eV was used. The Perdew−Burke−Ernzerhof (PBE) generalized gradient approximation[13] was used to calculate the exchange-correlation energy. A single *k*-point was used for Brillouin zone integration. The calculations were carried out within the canonical (NVT) ensemble, using a Nosé-Hoover thermostat[14,15] to control the temperature. The simulations were run at 25, 350, and 600 °C. Due to the high computational demand of these calculations, simulation times were restricted to about 4 ps. Although this is short by classical simulation terms, as shown below, it is long enough to make some important conclusions on this system.

3. Results

3.1. Water Structure. We tested the PBE approximation and the appropriateness of the pseudopotentials by calculating the average bond lengths and HÔH bond angle at 25 °C for bulk waters in our simulation cell. The results are given in Table 1. The intramolecular bond lengths and angles are in excellent agreement with the experimental results of Ichikawa et al.[16] at 25 °C. These were time-of-flight neutron-diffraction measurements on pure liquid water in the high-Q region at 25−200 °C. Our calculated HÔH angle is within 1% of the experimental value, while the OH bond length is correct to within 2%.

3.2. Radial Distribution Functions and Coordination. Atomic positions collected at each time step were used to construct the radial distribution functions (RDF) $g_{SrO}(r)$and $g_{SrH}(r)$. Although the short simulation times affect their quality, the peaks at different temperatures are clearly identifiable from each other. Longer times will improve the precision but not change the interpretation.

At 25 °C the Sr−O peak for the first hydration shell is clearly centered at about 2.6 Å (Figure 1). The calculated Sr−O distances are in excellent agreement with the experimental values of 2.63,[2] 2.62,[5] 2.61,[3] and 2.57 Å.[6] The running

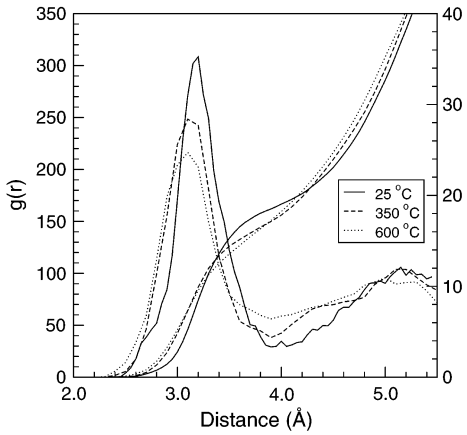

Figure 2. Calculated g(r) and n(r) for Sr−H at 25, 350, and 600 °C.

coordination number, integrated from the RDFs, is 7.6 at 25 °C. This also agrees very well with the experimentally measured values of 7.9,[17] 7.8,[6] and 7.3(5).[5]

The corresponding Sr−H peak (Figure 2) is centered at 3.2 Å. Although there are no experimental data to compare with, molecular dynamics simulations with classical potentials give a similar value of 3.3 Å.[6] The Sr−H coordination number at the minimum in the Sr−H radial distribution function is about 18.4. This is greater than twice the number of waters, suggesting that some hydrogens from the nonbonded waters are included in this.

Increasing the temperature to 350 °C causes the Sr−O bond length to contract by approximately 0.10 Å. This is somewhat larger than the 0.05 Å reduction measured by Seward et al.[6] over the temperature range 25−300 °C. The difference may be due to the higher temperature and density in our simulation or to the short runs. Nevertheless, the high-temperature peak is very clearly displaced toward the Sr ion and strongly supports the experimental data. There is a similar contraction in the Sr−H distance (Figure 2). There have been no experimental measurements of the Sr−H contraction yet.

As discussed briefly in the Introduction, classical molecular dynamics simulations failed to find a contraction[6,7] when using a rigid potential for water (SPC). Seward et al.[6] were able to predict a very slight contraction but only when using a flexible water potential, BJH.[18] However, this water potential predicted HOH angles of 101.2° under ambient conditions, which are quite different from the experimental values (about 106.6°). They also find from their simulations that the waters in the first hydration shell had slightly lower HOH bond angles of 99.1°. Our ab initio MD simulations predict HOH bond angles of about 107.6°, in better agreement with the experimental data. The hydrated waters show a very slight increase in bond angle, but given the small system and run times, this is probably not a significant result.

The running coordination numbers show a decrease from 7.6 at 25 °C to 6.7 at 350 °C (Figure 1). Seward observed a similar decrease in the coordination to 6.2 over the temperature range 25−300 °C,[6] while Pfund observed a greater change in the coordination to approximately 3.6 at 386 °C.[5] The much lower value of Pfund is likely due to the lower density of their solution, almost one-half the density of our simulation cell, rather than a temperature effect. The Sr−H coordination numbers also decrease, from 18.4 at 25 °C to 16.2 at 350 °C.

Increasing the temperature to 600 °C does not change the coordination further, and so we predict that Sr will remain octahedrally coordinated, even at these high temperatures.

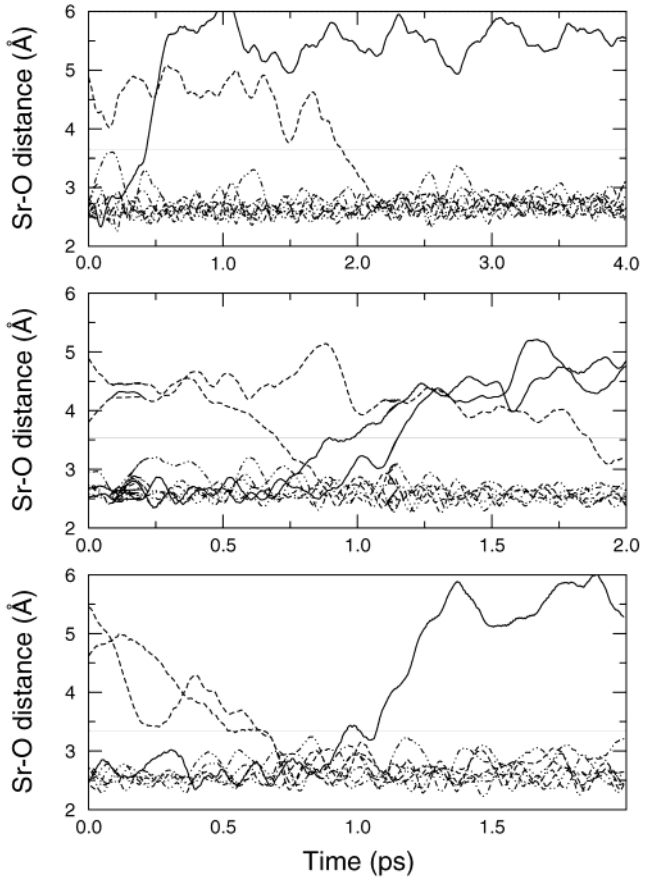

Figure 3. Calculated Sr−O separation at (a) 25, (b) 350, and (c) 600 °C. Horizontal gray line marks the closest approach of bulk waters to the Sr^{2+} ion. Dash−dot lines are first hydration shell waters. Solid lines are waters leaving the hydration shell. Dash lines are waters entering the hydration shell.

3.3. Hydration Shell Dynamics. The residence time for water in the Sr hydration shell is known to be very short ($<10^{-9}$ s), and this shows up well in our simulations (Figure 3). The solid line is the Sr−O distance for waters that leave the first hydration shell during the simulation, and the dashed line is for waters that enter the hydration shell from the bulk fluid. The other dot−dashed lines are Sr−O distances for waters that remain within the first hydration shell throughout the simulation. The bottom of the gray-shaded area denotes the nearest approach of the remaining bulk waters that do not enter the first hydration shell.

At 25 °C, the hydration shell is very well defined with a clear separation between this shell and the lower extent of the bulk waters (Figure 3a). Very early into the calculation one of the water molecules is ejected from the inner shell, as shown by the solid line in Figure 3a, and moved into the bulk water. The cluster remains 7-coordinate for 1.5 ps before a different second-sphere water moves into the first hydration shell. This gives an average coordination number of about 7.5, as already obtained from integrating $g(r)$.

The inner hydration shell remains identifiable at 350 °C; however, a water molecule is ejected from the shell during the equilibration stage of the calculation. As Figure 3b illustrates, this same ion moves back into the hydration shell within 1 ps; however, at the same time two other water molecules are lost. We examined the resulting structure and found that with the loss of these waters, the remaining six waters reorganize themselves into an octahedral arrangement. This rearrangement agrees well with the experiments of Seward et al.[6] Toward the end of the calculation, a water begins to approach the first hydration shell again.

Although it would be speculative to use these short simulations times to predict an average residency time or rate of exchange for waters in the hydration shell, they do show that the residency times are extremely short and on the order of 10^{-11} s.

We can, however, use this information to calculate a Debye−Waller factor for the hydrating waters by calculating the mean-squared displacement of a water in the first hydration shell from its average distance to the Sr ion. Using only waters that remain in the hydration shell throughout the simulation, we find an average Debye−Waller factor of 0.024 Å^2 at 25 °C and 0.036 Å^2 at 350 °C. These compare remarkably well with experimental values of 0.019 Å^2 at 25 °C and 0.030 Å^2 at 308 °C.[6]

Acknowledgment. We thank the E.P.S.R.C. for time on the T3E and Origin2000 at Manchester. We also thank the N.E.R.C for funding (GR3/12079).

References and Notes

(1) Neilson, G. W.; Broadbent, R. D. *Chem. Phys. Lett.* **1990**, *167*, 429−431.
(2) Persson, I.; Sandström, M.; Yokoyama, H.; Chaudhry, M. *Z. Naturforsch.* **1995**, *50a*, 21−37.
(3) Caminiti, R.; Musinu, A.; Paschina, G.; Pinna, G. *J. Appl. Crystallogr.* **1982**, *15*, 482−487.
(4) Alves Marques, M.; Cabaço, M. I.; de Barros Marques, M. I. Gaspar, A. M. *J. Phys.: Condens. Matt.* **2002**, *14*, 7427−7448.
(5) Pfund, D. M.; Darab, J. G.; Fulton, J. L.; Ma, Y. J. *J. Phys. Chem.* **1994**, *98*, 13102−13107.
(6) Seward, T. M.; Henderson, C. M. B.; Charnock, J. M.; Driesner, T. *Geochim. Cosmochim. Acta* **1999**, *63*, 2409−2418.
(7) Palmer, B. J.; Pfund, D. M.; Fulton, J. L. *J. Phys. Chem.* **1996**, *100*, 13393−13398.
(8) Berendsen, H. J. C.; Grigera, J. R.; Straatsma, T. P. *J. Phys. Chem.* **1987**, *91*, 6269−6271.
(9) Tongraar, A.; Liedl, K. R.; Rode, B. M. *J. Phys. Chem.* **1998**, *102*, 10340−10347.
(10) White, J. A.; Schwegler, E.; Galli, G.; Gygi, F. *J. Chem. Phys.* **2000**, *113*, 4668−4673.
(11) Payne, M. C.; Teter, M. P.; Allan, D. C.; Arias, T. A.; Joannopoulos, J. D. *Rev. Mod. Phys.* **1992**, *64*, 1045−1097.
(12) Refson, K. *Comput. Phys. Commun.* **2000**, *126*, 309−328.
(13) Perdew, J. P.; Burke, K.; Ernzerhof, M. *Phys. Rev. Lett.* **1996**, *77*, 3865−3868.
(14) Nosé, S. *Mol. Phys.* **1984**, *52*, 255−268.
(15) Hoover, W. G. *Phys. Rev. A* **1985**, *31*, 1695−1697.
(16) Ichikawa, K.; Kameda, Y.; Yamaguchi, T.; Wakita, H.; Misawa, M. *Mol. Phys.* **1991**, *73*, 79−86.
(17) Albright, J. N. *J. Chem. Phys.* **1972**, *56*, 3783−3786.
(18) Bopp, J. P.; Jancsó, G. Heinzinger, K. *Chem. Phys. Lett.* **1983**, *98*, 129−133.